



# Thermal power measurement of the novel evacuated tube solar collector and conventional solar collector during simultaneous operation



Radim Rybár, Martin Beer\*, Michal Cehlár

Department of Earth Resources, Faculty of Mining, Ecology, Process Control and Geotechnologies, Technical University of Košice, Letná 9, 042 00 Košice, Slovakia

## ARTICLE INFO

### Article history:

Received 17 December 2015

Received in revised form 25 February 2016

Accepted 25 March 2016

Available online 31 March 2016

### Keywords:

Thermal power measuring

Evacuated tube solar collector

Metal foam

Simultaneous operation

## ABSTRACT

The paper deals with a description of the measurement method and evaluation of the thermal power of evacuated tube solar collectors (ETSC) during their simultaneous operation at the Centre of Renewable Energy Sources, Technical University of Košice, Slovakia. Evaluation was performed during various climatic and solar irradiance conditions on experimental measuring apparatus, that was designed and manufactured by authors. Key feature of measuring apparatus is its ability to ensure simultaneous operation of both evaluated collectors. This method of operation was selected in order to ensure identical conditions for both evaluated solar collectors during all performed measurements. Within the evaluation were investigated two types of ETSC – one with a conventional manifold header, and the other with a parallel flow manifold header with metal foam structural element that was proposed by authors and it is under patent protection. The main objective of the comparison was to evaluate the effect of used metal foam structure and changes in inner configuration on the overall thermal power of the proposed solar collector through outdoor quasi dynamic test. Part of measurement was also devoted to pressure drop analysis of proposed prototype of manifold header. Within the presented measurements, ETSC with parallel flow manifold header with metal foam structural element demonstrated significant thermal power increase ranging from 85.2 to 201.8 W per 1 m<sup>2</sup> of collector area (depending on used flow rates of heat transfer medium) and increase of performance enhancement factor in range from 1.14 to 3.20.

© 2016 Elsevier Ltd. All rights reserved.

## 1. Introduction

Despite the fact that renewable energy sources are characterized by time variation [1], geographic isolation [2] and dependency on climatic conditions [3], they certainly are one of the greatest catalyst of human society development in present [4]. Technical potential of using solar energy for the energy demand of human society is one of the largest [5,6], which corresponds to a wide range

of technical application in field of the solar energy. Production of heat with use of solar energy takes place in various ways using simple liquid solar collectors, ETSC with heat pipes or structurally more complex hybrid photovoltaic–thermal collectors [7]. Flat plate solar collectors that were massively used in the past are now being replaced by ETSCs [8], which achieve higher thermal efficiency and hence heat gain. Use of heat pipes is widespread in various industries – refrigeration applications, electrical engineering, space technology, and not at least in the solar thermal applications [9]. ETSCs consists of two relatively simple structural parts – evacuated tube heat pipes and manifold

\* Corresponding author. Tel.: +421 55 602 2398.

E-mail address: [martin.beer@tuke.sk](mailto:martin.beer@tuke.sk) (M. Beer).

## Nomenclature

$A$	aperture of solar collector ( $\text{m}^2$ )
$P$	power per collector area unit (W)
$P_{\text{CP}}$	performance of circulation pump (W)
$T$	temperature (K)
$U_p$	uncertainty of power per collector area unit (%)
$Q$	volumetric flow rate ( $\text{m}^3 \text{s}^{-1}$ )
$c$	specific heat capacity ( $\text{J kg}^{-1} \text{K}^{-1}$ )
$\dot{m}$	mass flow rate ( $\text{kg s}^{-1}$ )
$p$	pressure (Pa)

### Greek symbols

$\Delta$	difference (–)
----------	----------------

$\delta$	uncertainty of measured value (–)
$\theta$	collector tilt angle ( $^\circ$ )

### Abbreviations

ETSC	evacuated tube solar collector
I	in
MF	metal foam
O	out
PPI	pores per inch
S	standard

header of solar collector. Functional principle of the ETSC uses a simple physical phenomenon of the phase change of the working fluid flowing in the body of the heat pipe. As a result of increased temperature (due to the solar irradiance) working fluid evaporates and rises in the centre of the pipe to her top, where in the condenser section (with pressure and temperature changes) condenses and in the capillary structure form on the tube wall flows to the lower part of heat pipe where the evaporation cycle restarts again. Released heat is removed by manifold header, where heat pipes are inserted and by heat transfer medium to the solar hydraulic circuit and for further use. Heat pipe is supplemented with thin absorber plate that absorb solar radiation and transfers heat to the working fluid. Heat pipe with absorber is placed in evacuated glass tube that serves as a thermal insulation.

Notwithstanding the fact, that ETSC are technologically highly-efficient devices for conversion of solar radiation into useful heat (in the form of hot water), the possibility of innovation of this devices is still relatively high. Liu and Li [10] in their work evaluated the use of nanofluids in heat pipes. Authors reported that for the majority of heat pipes adding nanoparticles to the working fluid increases the efficiency of heat transfer, reducing thermal resistance and increases heat removal capacity. Peng et al. [11] in published work proposed a new type of heat pipe, which consists of flat evaporation and condensation section, and perforated aluminium inner ribs that forming the capillary structure. The outer part of condensation section was supplemented with several coolers. Peng et al. report, that this modularly constructed heat pipe effectively cools electrical equipment with 100 W output and surface temperature 60 °C. Authors also noted acceleration of phase change process, and therefore the beginning of the cooling.

In the field of using heat pipes in solar thermal technology are innovation applied directly in technical design or arrangement of the heat pipes, and authors lesser deal with other parts of ETSC such as manifold headers. Chen et al. [12] designed and manufactured evacuated tube heat pipe for solar collector, which outer insulation shell was made of acrylic tube. Acrylate is not only cheaper material than glass, but its ability to resists mechanical damage is much greater. However, heat pipe with acrylate outer shell has

15% greater heat loss than heat pipe with glass outer shell. Rassamakin et al. [13] in presented work proposed heat pipe made of extruded aluminium alloy, which reduced its weight. Authors also proposed changes of inner cross-sectional shape of heat pipe in form of wider spacing in the longitudinal slots of the capillary structure, which prevent backflow of the working fluid. After incorporation of these changes, authors experimentally determined the overall benefit of innovation during thermal efficiency measurement of ETSC, when upgraded ETSC reached value of thermal efficiency 0.72 and single tube had thermal power 210 W. Robinson and Sharp [14] proposed modifications of heat pipes that are characterized by change of copper absorber and all soldered joints between absorber and evaporation section. Authors also implemented new rubber adiabatic section and thicker insulation. The contribution of modification was evaluated in form of solar fraction parameter, when solar collector with modified heat pipes increased value from 62.5% to 89.2%. Moradgholi et al. [15] in published work presented innovative photovoltaic-thermal solar collector, which used heat pipes (thermosyphons) for cooling of photovoltaic cells. Authors was able to decrease temperature of photovoltaic cells about 15 °C and increase solar collector efficiency (including thermal efficiency) about 15.3% (spring) and 44.3% (summer). Deng et al. [16] proposed flat plate liquid solar collector with micro-channel heat pipe array. This new type of solar collector showed about 25% higher thermal efficiency than conventional flat plate solar collectors.

Use of metal foam for solar thermal application is relatively widely adopted. Wang et al. [17] analyzed suitability of solar driven  $\text{CO}_2$  methane reforming process in metal foam reactor. The same author also published paper [18] where numerically analyzed the possibility of use metal foam as a reactor in process of hydrogen production via methane steam reforming method, where as a heat source was used solar concentration element.

Large number of authors previously dealt with evaluation of various types of solar collectors. Tests of the solar collectors can be divided into two groups, first group contains tests when authors evaluate solar collectors according their efficiency curve, second group contains test when solar collectors are evaluated according their

thermal power or heat gain. Another selection divides test of the solar collectors on test that are conducted in laboratory conditions, when solar collectors are tested under steady state conditions and on test that are conducted under dynamically changing outdoor conditions. Methods of solar collector testing are directly regulated by several technical standards, EN 12975-2 [19], ASHRAE 93 [20], ISO 9806-1 [21], GB/T18708-2002 [22] and GB/T 19141-2011 [23]. Within this standards are measurement conditions for laboratory and outdoor tests strictly specified.

Sabiha et al. [24] in published work performed tests of ETSC, that used single walled carbon nanotubes nanofluid as an heat transfer medium. Authors used in-house manufactured experimental measuring apparatus and recorded values of volumetric flow rate and temperature of heat transfer medium, and intensity of solar irradiance. Resulting evaluation of solar collectors was done by means of calculation of the thermal efficiency. Similar methods used Hayek et al. [25] while they used conventional ETSC. Colangelo et al. [26], used combination of nanofluids and flat plate liquid solar collector, which test was performed under technical standard EN 12975-2 in laboratory and also outdoor conditions. Authors evaluated solar collector in form of thermal efficiency. Liang et al. [27] in published work dealt with new type of photovoltaic–thermal solar collector with graphite layers, that ensure effective distribution of heat from photovoltaic cells to the heat transfer medium. Authors described outdoor test, in which they measured electrical and thermal parameters of the solar collector. Resulting evaluation was done by comparison of the thermal and electrical efficiency. Outdoor test of the hybrid photovoltaic–thermal collector with similar method was also performed by Shan et al. [28]. Joshi and Jani [29] performed laboratory measurement of the thermal efficiency of solar cookers. Visa et al. [30] developed new type of flat plate liquid solar collector with trapezoid shape, that can be used as an integral part of modern building facade. Result of laboratory and outdoor measurements was in form of the efficiency curve of the proposed solar collector. Osório and Carvalho [31] compared on sample of five solar collectors (two flat plate liquid and three ETSC) suitability of quasi dynamic method of testing and steady state testing under technical standard EN 12975-2. Results of test had form of efficiency curves of five solar collectors for both evaluated methods. Du et al. [32] in their work proposed experimental testing platform for laboratory and outdoor test of ETSC, with this platform authors evaluated conventional ETSC in form of thermal efficiency and incidence angle modifier. Similar measuring rig was proposed by Yang et al. [33]. Their system consists of sun tracking flat mirror reflector system that allows optimization of insolation condition of evaluated solar collector.

Testing of the solar collectors, resp. solar thermal system with using of thermal power evaluation is also frequently used method. Advantage of this method is characterized by low demand on the measurement instrumentation [34] and in certain cases by higher accuracy of the results, since a smaller number of measurement instrumentation (with given uncertainty) generates less error propagation in the results of measurement. This method of testing is used to evaluate overall thermal power of solar

thermal system, respectively to evaluate solar applications, which do not need to be evaluated according to the efficiency curve. Ayompe and Duffy [35] in their work evaluated thermal power of ETSC during the trial outdoor operation while they measured values of volumetric flow rate and temperature of heat transfer medium, ambient climatic conditions and solar irradiance intensity. The final evaluation was done by analysis of thermal power and heat gain of the solar system for a specified time period. Geddam et al. [36] in presented work measured thermal power of solar cookers in outdoor tests. Zambolin and Del Col [37] compared thermal power of two solar collectors – flat plate liquid solar collector and ETSC in outdoor test under technical standard EN 12975-2. Besides the measurement of the thermal efficiency, authors also measured heat gain of the solar collectors.

In presented work, evaluation of ETSCs is based on both mentioned methods. Measurement of thermal power was carried out under quasi dynamic conditions with varying volumetric flow rate of the heat transfer medium, with changing ambient conditions (velocity, humidity and temperature of air) and with changing solar irradiance intensity. Simplification of the measurement process and from this resulting reduction of measurement instrumentation proportionally contributes to increase of absolute accuracy of comparison of the conventional ETSC and ETSC with parallel flow manifold header with metal foam structural element proposed by authors.

## 2. ETSC manifold header – object of innovation

Fig. 1 depicted object of innovation – manifold header of ETSC. In the figure is clearly visible inner configuration of standard manifold header and proposed parallel flow manifold header with metal foam structural element. Standard manifold headers are structurally simple devices. Body of manifold header usually consists of the thin walled copper tube of larger diameter (approximately 30 mm) with soldered inlet and outlet pipes. Heat pipe condenser casings are manufactured from copper pipes of a smaller diameter (10–20 mm, according to the size of condenser) and length of 100 mm. Casings are inserted and soldered into holes, which dimensions and spacing depends on the number and type of used heat pipes. Heat transfer medium flows through the inlet pipe to the body of manifold header where gradually washes each heat pipe condenser casing and remove heat from condenser. Heated heat transfer medium afterward flows through outlet pipe to hydraulic circuit for further demand. The main disadvantage of this configuration is the non-uniform heat remove from condenser, i.e. each condenser casing is washed by heat transfer medium with different, gradually increased temperature, what resulting to the reduced effectiveness of heat exchange and also the operating conditions of heat pipes are uneven, what caused their uneven wear (thermal degradation). Another negative factor is relatively large liquid volume of manifold header, that caused impaired reactions of manifold header (high value of thermal inertia) to the dynamically changing intensity of solar irradiance (e.g. days with intermittent cloud covered sky).

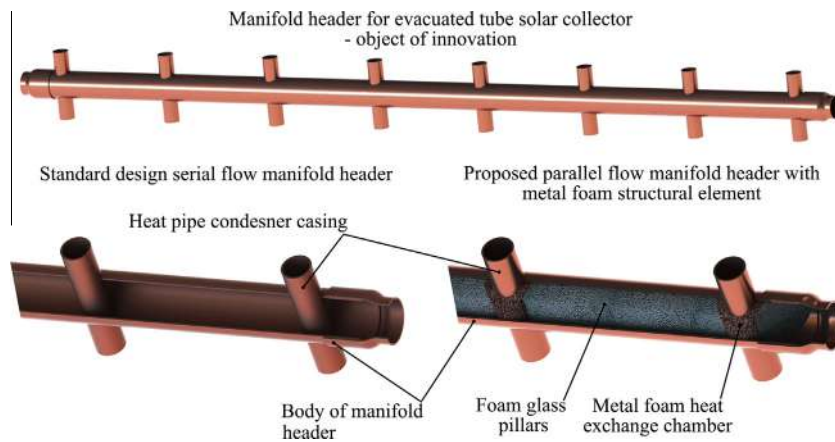


**Fig. 1.** Comparison of inner configuration of standard manifold header and proposed parallel flow manifold header with metal foam structural element.

Manifold header proposed by authors eliminates not only identified disadvantages of standard manifold headers by changing flow conduction to condensers, but it also increases heat exchange efficiency. Presented innovation is characterized by implementation of new structural parts in the form of heat exchange chambers made of metal foam and blocks of foam glass, that allows change of flow conduction from disadvantageous serial flow to more advantageous parallel flow. Fig. 2 depicts flow vectors and principle of flow conduction to the condenser casing for standard manifold Fig. 2(A), and for proposed innovative manifold header Fig. 2(B).

Blocks of foam glass create flow channels in such shape and configuration, that the condenser casing are separately washed by heat transfer medium at the same temperature. The same temperature of heat transfer medium at the condenser ensures identical operating conditions and thus identical wear of heat pipes. Flowing heat transfer medium enters the manifold header through inlet pipe and afterward flows through distribution channel of manifold header. Dimensions of distribution channel are gradually reduced, so from the hydraulic point of view it occurs to diagonal division of the flow to each condenser casing (see Fig. 2). Resulting partial flows washed condensers in

heat exchange chambers and afterward heat transfer medium flows through collection channel to the outlet pipe. Dimensions of body of the manifold header and condenser casing are identical to standard manifold header, but with change of inner configuration the inner liquid volume of manifold header decreases from 450 ml to 135 ml.

Cylindrical blocks of foam glass, that creates flow channels, have length of 120 mm and a diameter of 26 mm. The edges of the cylinder are dimensionally adapted to the shape of the heat exchange chambers. In longitudinal directions are block of foam glass machined in way that distribution flow channel is gradually reducing and collection flow channel is gradually expanding. The use of foam glass is suitable because of its properties, such as hydrophobicity, resistance to high temperature (up to 450 °C) and low heat conductivity ( $<0.045$  W/m K). An interesting and environmentally positive features of the foam glass is its origin in recycling process of waste glass. Proposed manifold header contains seven blocks of foam glass, and two blocks that forming inlet and outlet part.

Heat exchange chambers of proposed manifold header (see Fig. 1) are made of unique porous material – metal foam. Metal foam consists of a network of interconnected fiber of base material (metal), which forms pores and cells

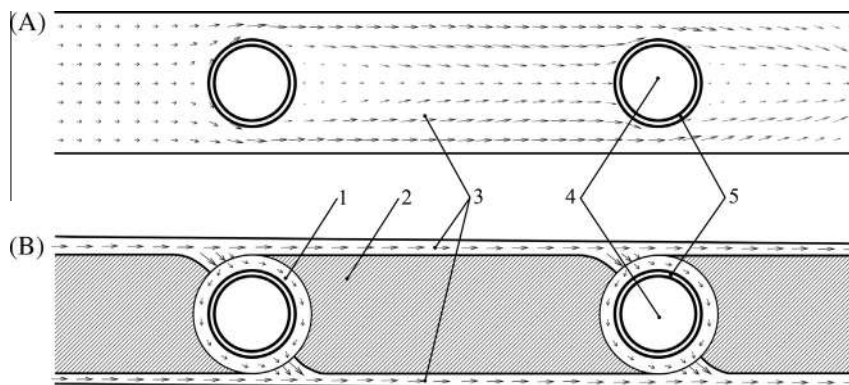


**Fig. 2.** Difference between flow canals in standard manifold header (A) and proposed innovative manifold header (B) with depicted flow vectors and inner parts (1 – metal foam heat exchange chamber, 2 – foam glass pillar, 3 – flow channels, 4 – heat pipe condenser, 5 – condenser casing).

that are permeable to liquid or gaseous medium. From the perspective of use in heat exchange application is its key feature a specific surface area. It is surface area that are formed by the sum of the areas of all microscopic fibers and their crosses (metal foam struts). The specific surface area is the interface area between liquid or gaseous medium and a solid phase of metal foam, it is a surface that is directly involved in heat exchange process. Higher value of specific surface area implies higher coefficient of heat transfer. Values of specific surface area can varies in range from 300 to 10,000 m<sup>2</sup> m<sup>-3</sup>. According to some open literature, Bai and Chung [38], Boomsma et al. [39], use of the metal foam in the heat exchangers significantly increases heat transfer coefficient, or heat transfer efficiency of devices. Another important properties of metal foam is pore density, respectively number of pores per inch (PPI). Pore density effects on permeability and pressure loss of the flowing medium. Values of pore density varies in range from 5 to 80 PPI. Use of metal foam in form of heat exchangers, filters, flow mixers, sound and impact absorbers or catalyst beds has a long history. Chumpia and Hooman [40] investigated the specific thermal properties of the foam metal used as a heat exchanger. Zhou et al. [41] used metal foam structure as a capillary structure on inner wall of heat pipe. Dyga and Placzek [42] investigated heat transfer of metal-fluid system, respectively possibility of use metal foam as a heat exchanger [43].

Heat exchange chamber of proposed manifold header has shape of annulus with outer diameter of 24 mm, and inner diameter of 16 mm. Annulus has height 26 mm. Cross-sectional shape of annulus is fitted to circle diameter of 26 mm, same as the body of manifold header. Heat exchange chambers are made of copper metal foam of thickness 4 mm and pore density 20 PPI with relative density 300 kg m<sup>-3</sup>. Specific surface area of used metal foam is approximately 1400 m<sup>2</sup> m<sup>-3</sup>, it means that each heat exchange chamber has fluid–solid interface area of 0.0075 m<sup>2</sup>, standard manifold has fluid–solid interface area only 0.0012 m<sup>2</sup>. This comparison shows that use of metal foam as a heat exchange chamber increases fluid–solid interface about 625%. Proposed innovative manifold header contains eight heat exchanger chambers, since we used ETSC with eight evacuated tube pipes.

Described proposal of manifold header resulting to the manufacturing of functional prototype of parallel flow manifold header with metal foam structural element. Prototype was manufactured in-house by authors, since authors have a long experience with manufacturing of heat devices [44,45]. Prototype was used as a part of the ETSC during experimental trial operation at Centre of Renewable Energy Sources, Technical University of Košice, Slovakia.

### 2.1. Pressure drop analysis of manifold header

In applications using metal foam is pressure drop always crucial parameter. Pressure drop analysis of proposed prototype was carried out before its installation into the solar collector. The aim of the analysis was to determine the pressure loss of manifold header and calculate required power increase of circulation pump, that have to compensate increase of pressure loss. Pressure drop of pro-

posed manifold header is caused by a flow of heat transfer medium through narrowed flow channels and heat exchange chamber made of metal foam. Measurement of pressure drop of prototype was carried out with using a measuring apparatus type AMI300 with pressure module (accuracy 0.2% full scale) from manufacturer Kimo instrument (see Fig. 3).

Within the measurements were used the same mass flow rates of heat transfer medium (in this case water) which were planned during experimental trial operation of entire solar collector, i.e. 0.016, 0.033 and 0.061 kg s<sup>-1</sup>. Measurement of pressure drop was performed on both manifold headers – on parallel flow manifold header with metal foam element and on standard manifold header from manufacturer SUNDA SOLAR. Fig. 4 depicted graphical comparison of pressure drop of both manifolds.

The comparison showed that the prototype of manifold header has approximately three times greater pressure loss than standard manifold header. For the mass flow rate of 0.016 kg s<sup>-1</sup> is pressure loss of prototype higher about 1256 Pa, for 0.033 kg s<sup>-1</sup> about 3090 Pa, and for 0.061 kg s<sup>-1</sup> about 7469 Pa. Based on the Bernoulli's equation was calculated required power increase of circulation pump (Eq. (1)), where  $\Delta p_{(MF-S)}$  is difference between pressure loss of prototype and pressure loss of standard manifold header and  $Q$  is volumetric flow rate of heat transfer medium.

$$P_{CP} = Q \cdot \Delta p_{(MF-S)} \quad (1)$$

For the mass flow rate of 0.016 kg s<sup>-1</sup> is required increase of pump power 0.02 W, for 0.033 kg s<sup>-1</sup> it is 0.10 W, and for 0.061 kg s<sup>-1</sup> it is 0.45 W. In comparison with used circulation pump with 60 W input, these values of required increase represents only 0.03%, 0.16% and 0.75% of this value. Low values of pressure drop and thus required increase of pumping power are caused by several factors, but mainly by used volumetric flow rate of heat transfer medium and by used type of metal foam. In the case of proposed prototype of manifold header was used highly permeable metal foam with pore density of 20 pore per inch and with relatively large pore diameter of 2.262 mm. Condenser casings were enveloped with a layer of metal foam with thickness of only 4 mm (so amount of metal foam in used prototype is small). A more significant parameter influencing the pressure drop is volumetric flow rate of used heat transfer medium. In the case of presented experimental solar system were used mass flow rates in the range from 0.016 to 0.061 kg s<sup>-1</sup> (respectively the volumetric flow rates  $1.6 \times 10^{-5}$ ,  $3.3 \times 10^{-5}$  and  $6.1 \times 10^{-5}$  m<sup>3</sup> s<sup>-1</sup>). The low values of pressure loss are also achieved by the inner configuration of manifold header where structural parts creates conditions for parallel flow of heat transfer medium. After consideration of these fact, it can be concluded that using of prototype of manifold header have insignificant impact on increase of pressure drop.

### 3. Experimental setup and measurement method

Contribution of the proposed innovation on total heat gain of the solar collector was quantified during



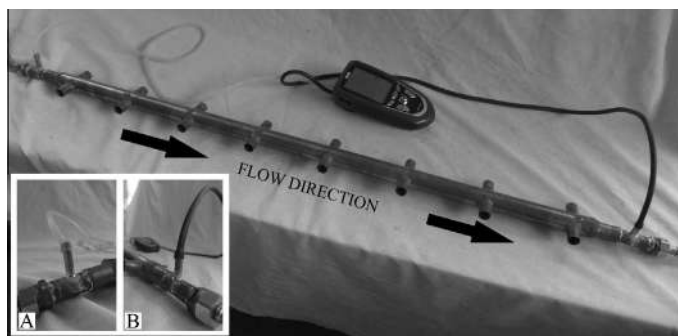


Fig. 3. Measuring of pressure drop (A – inlet probe, B – outlet probe).

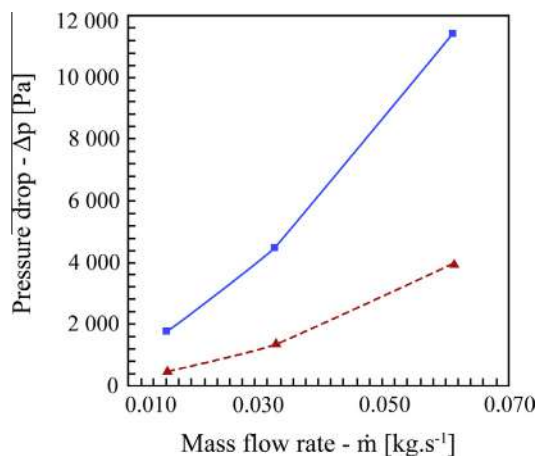


Fig. 4. Graphical representation of pressure drop.

simultaneous operation of two ETSCs with their mutual comparison. As a basis of comparison were used two ETSCs of manufacturer SUNDA SOLAR with eight evacuated tube heat pipes. Outer shell of used evacuated tube heat pipe was made of borosilicate glass tube with outer diameter of 140 mm, length 1980 mm and wall thickness of 2.2 mm. Inside the tube formed vacuum ( $5 \times 10^{-3}$  Pa) provides thermal insulation. Heat pipe consists of copper thin wall tube, evaporation section has length 1890 mm and diameter of 8 mm, condensation section at the top of heat pipe has length 70 mm and diameter of 14 mm. As working fluid was used water. Heat pipe is placed inside of borosilicate glass tube. Aluminium absorber of heat pipe has thickness of 0.47 mm and aperture 0.28 m<sup>2</sup>. Absorber surface has selective coating made of aluminium nitride (absorptance > 0.94, emittance < 0.06). Total aperture (A) of used solar collector has 2.23 m<sup>2</sup>. Stagnation temperature of heat pipe is determined on 247 °C, respectively on 190 °C for whole solar collector. ETSCs, on which comparison was performed had identical evacuated tube pipe and thermal insulation, their difference lays only on used manifold header. First solar collector used standard (commercially available) manifold header (hereinafter ETSC 1-S), second solar collector used proposed and manufactured parallel flow manifold header with metal foam structural element (hereinafter ETSC 2-MF).

Simultaneous experimental operation of described solar collectors ETSC 1-S and ETSC 2-MF was realized at the Centre of Renewable Energy Sources, Košice, Slovakia (latitude 48°43'N and longitude 21°15'E). Because of the space restrictions of the Centre of RES it was necessary to design solar system on mobile platform suitable for personal manipulation.

Result of these restrictions is design of experimental measuring apparatus (see Fig. 5), which consists of two structurally independent parts used for attaching of evaluated solar collectors. For every time, when experimental apparatus was installed out of the Centre RES were both parts handled separately. Framework of each part was manufactured from rectangular steel pipes with dimensions 20 × 20 mm, height of framework is 2150 mm, width 900 mm and depth 500 mm. According to required measurement conditions, tilt angle of collectors was set to 75°. Except solar collectors, both frameworks were supplemented with parts of hydraulic circuit. Hydraulic system was designed and manufactured in order to allow disconnection of pipes without loss of liquid or forming of air pocket, since disconnection of pipes was necessary in the process of handling with experimental measuring apparatus. Hydraulic system consists of the following components – polypropylene distribution pipes and fittings with diameter of 20 mm, rubber-based thermal insulation Armaflex (thermal conductivity under 0.035 W/m K), expansion tank Zilmet Inox-pro with volume of 4 l and maximum operation pressure 500 kPa, electric circulation pump AquaCUP GRS 25-40 with a variable output 90–60–40 W, spiral counter flow heat exchanger Stiebel, set of regulation valves, on-off valves, set of air vents, brass reducer and fittings. As a heat transfer medium was used water. Schematic diagram of experimental measuring rig with hydraulic system, basic parts and position of measurement instrumentations is depicted in Fig. 6.

Heat transfer medium flows from electric circulation pump to the T – distributor of cold water section, where pipe is divided and heat transfer medium flows separately to each manifold headers. In each manifold headers, temperature of heat transfer medium increases. Heated heat transfer medium flows through T – distributor of hot water section, where separated flows are mixed and afterward flows to the counter flow spiral heat exchanger where is gained heat delivered for further usage. Possible pressure

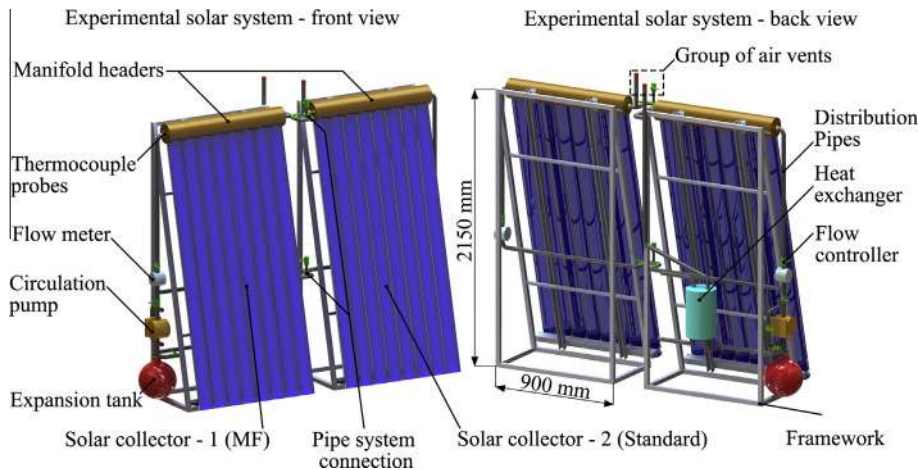


Fig. 5. 3D renderings of designed and manufactured experimental measuring apparatus.

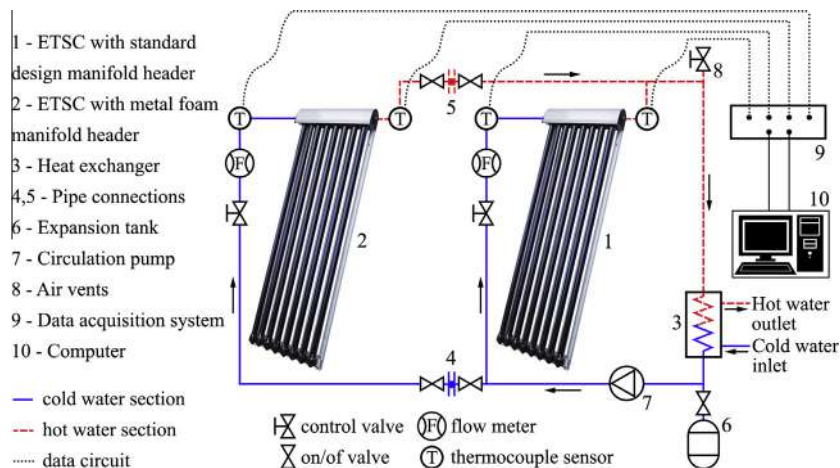


Fig. 6. Schematic diagram of experimental setup.

changes of heat transfer medium caused by the change of temperature are compensated by expansion tank that is installed at the lowest point of the hydraulic circuit. Important part of hydraulic system are pipe joints, that allow disconnection of hydraulic system and manipulation with both part of experimental measuring apparatus separately. Air vents are placed at the highest part of the hydraulic system.

Hydraulic system is supplemented with measurement instrumentation in form of four thermocouple probes and two flow meters (see Fig. 7). Thermocouple probes type TTKE-363 from manufacturer Kimo instruments (type K, range  $-40^{\circ}\text{C}$  to  $+400^{\circ}\text{C}$  with accuracy  $\pm 0.01^{\circ}\text{C}$ ) was installed before and after each manifold header in special housing with metric thread M8. The purpose of the thermocouple probes were recording the temperature difference of heat transfer medium, before and after leaving manifold header. Data from thermocouples were recorded with data acquisition system type AMI 300 from manufacturer Kimo instruments with data logger, which was connected with personal computer. Volumetric flow rate of

heat transfer medium was measured with two mechanical differential pressure direct reading flow meter type SMART +JS-02 from manufacturer Apator (with accuracy  $(\pm 5\% \text{ full scale})$ , which were placed after 1 in. control valves and before each individual manifold headers.

The procedure of thermal power measuring consists of a series of steps, that started with installation of evaluated solar collector outside of Centre RES (see Fig. 8), followed with interconnection of distribution pipes of hydraulic systems, testing its function and potential leakages. Afterward, secondary cooling system was connected to counter flow spiral heat exchanger. Final step was devoted to setting of required volumetric flow rate of heat transfer medium and starting of measuring instruments. After finishing of the measurements and recording of measured values, it was necessary to manually disconnect hydraulic system, and carry two separated parts in the interior of Centre RES.

Comparison of the evaluated ETSC was performed during spring, respectively early summer months under quasi dynamic conditions, with changing values of ambient con-

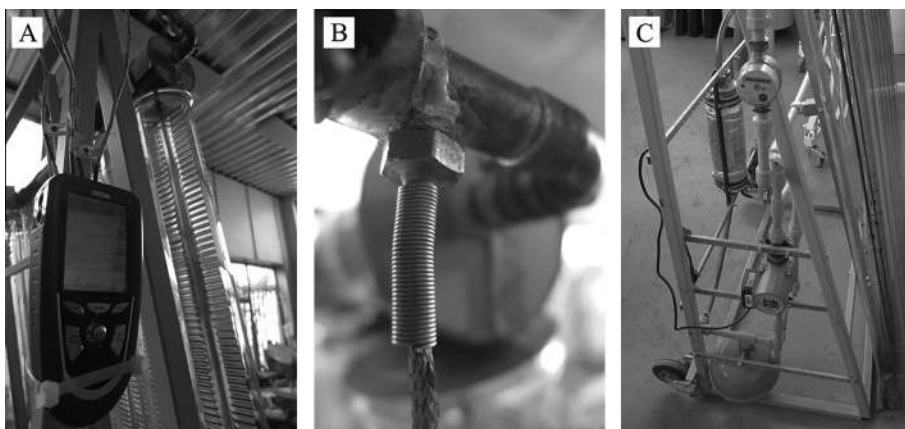


**Fig. 7.** Detailed view of the measurement instruments (A – data acquisition system AMI 300 with plugged thermocouple probes, B – position of thermocouple probes, C – part of hydraulic system with circulation pump, flow meter and regulation valve).



**Fig. 8.** ETSC 1-S and ETSC 2-MF during operation at Centre of Renewable Energy Sources, Košice, Slovakia.

ditions (temperature, humidity and velocity of air) and with changing values of solar irradiance intensity, from clear to intermittent cloud covered sky. Within the test it was performed six sets of measurement with duration 150 min (with data interval 10 s), from which representative sample are presented (TEST 1 to TEST 4 in Section 5). Previously described ETSCs were compared at different volumetric, respectively mass flow rate. As a basic flow rate was used value of  $0.033 \text{ kg s}^{-1}$ , which is recommended by manufacturer SUNDA SOLAR. Other used mass flow rates had value of  $0.016 \text{ kg s}^{-1}$  (half of recommended value) and value of  $0.061 \text{ kg s}^{-1}$  (almost double of recommended value). Table 1 depicted summary factors of presented method of measurement.

During measurement process were not recorded values of solar irradiance intensity or parameters of surrounding environment (ambient temperature, humidity and wind speed), since the evaluation of ETSCs was performed only

**Table 1**

Summary of used measuring method.

Parameter	Values	Unit
ETSC aperture, $A$	2.23	$\text{m}^2$
ETSC tilt angle, $\theta$	75	$^\circ$
Method of testing	Outdoor quasi dynamic	/
Working fluid	Water	/
Working fluid mass flow	0.016 0.033 0.061	$\text{kg s}^{-1}$

as a comparison of their thermal power. Influence of environment and solar irradiance intensity was on both evaluated solar collectors identical, and thus may be neglected. The only different parameters of evaluated solar collectors were used manifold headers. Used method with reduced number of measurement instrumentations and thus inputs of calculations does not degrade informative value of presented comparison of the solar collector. A smaller number of input values of calculation reduces error propagation to the final comparison and then informative value of the comparison rises.

#### 4. Data and uncertainty analysis

As an output parameters of comparison were used values of thermal power per collector are unit of the ETSC 1-S (Eq. (2)), and of the ETSC 2-MF (Eq. (3)). Inputs of Eq. (2), respectively Eq. (3) were values of temperature difference ( $\Delta T$ ), mass flow rate ( $\dot{m}$ ), specific heat capacity of water ( $c$ ) and aperture area of solar collector ( $A$ ).

$$P_S = \frac{\dot{m} \cdot c \cdot \Delta T_S}{A} \quad (2)$$

$$P_{MF} = \frac{\dot{m} \cdot c \cdot \Delta T_{MF}}{A} \quad (3)$$

In the measurement process were recorded values of temperature of the heat transfer medium before entering of manifold header  $T_{MF,i}$ , respectively  $T_{S,i}$ , and after leaving manifold header  $T_{MF,o}$ , respectively  $T_{S,o}$ . These temperatures were used as an inputs for temperature difference calculation  $\Delta T_{MF}$ , respectively  $\Delta T_S$  in Eqs. (4) and (5).



$$\Delta T_{MF} = T_{MF,O} - T_{MF,I} \quad (4)$$

$$\Delta T_S = T_{S,O} - T_{S,I} \quad (5)$$

Values of mass flow rate ( $\dot{m}$ ) was set and recorded for each test separately, value of specific heat capacity ( $c$ ) was determined according to temperature of heat transfer medium, aperture area of the solar collector ( $A$ ) was determined according to technical documentation from manufacturer and verified with precise tape measure by authors.

Uncertainty of measurement and error propagation were analyzed with Kline–McClintock method [46] according Eq. (6). Analysis involved uncertainty of thermocouple probes ( $\pm 0.01^\circ\text{C}$ ), uncertainty of data acquisition system ( $\pm 0.8^\circ\text{C}$ ), uncertainty of reading and regulation of mass flow rate ( $\pm 5\%$  full scale, according to manufacturer), and uncertainty of measurement of solar collector aperture, which was measured with precise tape measure with uncertainty  $\pm 1.1\text{ mm}/10\text{ m}$ .

$$U_p = \sqrt{\left(\frac{\delta T}{T}\right)^2 + \left(\frac{\delta \dot{m}}{\dot{m}}\right)^2 + \left(\frac{\delta A}{A}\right)^2} \times 100\% \quad (6)$$

Result of the uncertainty analysis shows that the average uncertainty of thermal power per collector area unit is  $\pm 1.9\%$  with maximum value  $\pm 2.8\%$ .

## 5. Results and discussion

Evaluation of two solar collector was performed by comparison of their thermal power per collector area unit

and by definition of performance enhancement factor of the proposed manifold header. This methods were selected as most suitable methods for quantification of contribution of proposed innovation on overall thermal power of solar collector. Presented results represent selection of all performed measurements. Data reduction was performed in order to increase the clarity of the comparison. For the purposes of comparison were selected four sets of measurement labeled as TEST 1 to TEST 4, which was performed under different climatic conditions and with different mass flow rate of heat transfer medium.

First measurement, labeled as TEST 1 (see Fig. 9), was performed with the highest mass flow rate  $0.061\text{ kg s}^{-1}$ . This highest mass flow rate, nearly double of the recommended value by manufacturer of solar collector, was chosen with intent to test proposed manifold header beyond boundaries of normal operation. In this measurement ETSC 2-MF reached higher value of thermal power per collector area unit against ETSC 1-S, in average  $1116.1\text{ W m}^{-2}$  against  $914.3\text{ W m}^{-2}$ , e.g. thermal power increase was  $201.8\text{ W m}^{-2}$  (18.07%).

Second measurement, labeled as TEST 2 (see Fig. 9), was performed with mass flow rate  $0.033\text{ kg s}^{-1}$ , which represents standard used mass flow rate for similar types of solar collectors. In this measurement ETSC 2-MF reached higher value of thermal power per collector area unit against ETSC 1-S, in average  $696.8\text{ W m}^{-2}$  against  $611.6\text{ W m}^{-2}$ , e.g. thermal power increase was  $85.2\text{ W m}^{-2}$  (12.22%).

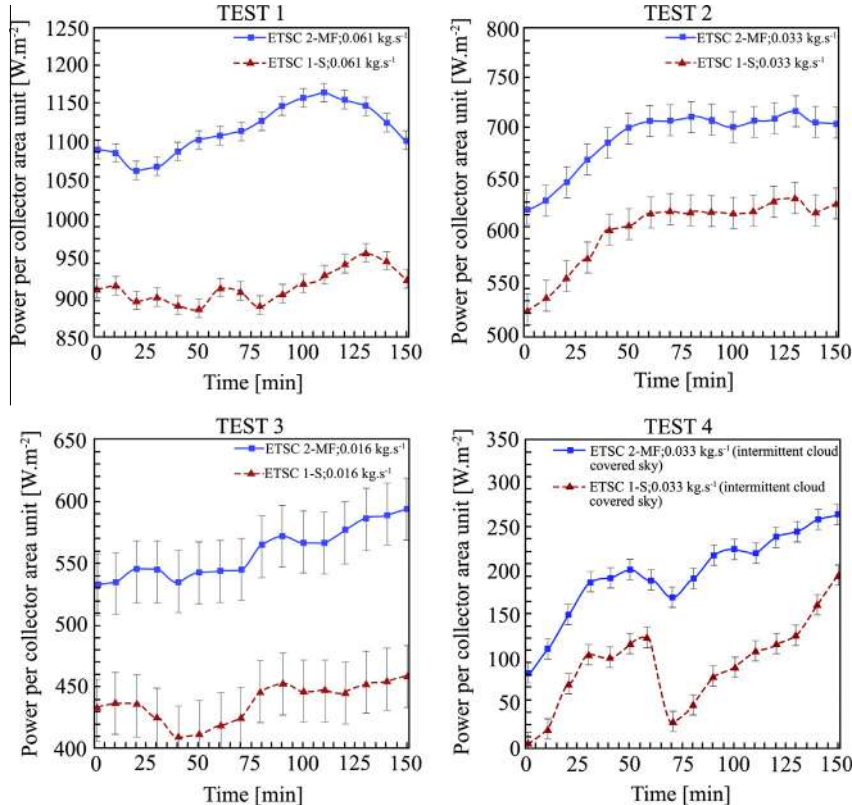


Fig. 9. Summary view of comparison of the thermal power per collector area unit for TEST 1 to TEST 4 (with depicted uncertainty error bars).

Third measurement, labeled as TEST 3 (see Fig. 9), was performed with mass flow rate  $0.016 \text{ kg s}^{-1}$ , which represents half of recommended value. In this measurement ETSC 2-MF reached higher value of thermal power per collector area unit against ETSC 1-S, in average  $562.7 \text{ W m}^{-2}$  against  $441.2 \text{ W m}^{-2}$ , e.g. thermal power increase was  $121.5 \text{ W m}^{-2}$  (21.59%).

Fourth measurement, labeled as TEST 4 (see Fig. 9), depicted operation of solar collector during day with intermittent cloud covered sky. TEST 4 was performed with mass flow rate  $0.033 \text{ kg s}^{-1}$ . In this measurement ETSC 2-MF reached higher value of thermal power per collector area unit against ETSC 1-S, in average  $197.3 \text{ W m}^{-2}$  against  $95.0 \text{ W m}^{-2}$ , e.g. thermal power increase was  $201.8 \text{ W m}^{-2}$  (51.81%).

As can be deduced from Fig. 9, period of this measurement began at the time when solar irradiance reached lower values due to intermittent cloud covered sky. In such a disadvantageous conditions ETSC 2-MF was able to reach higher values of thermal power, while ETSC 1-S was unable to produce significant thermal power. After an increase of the solar irradiance intensity, thermal power of both evaluated solar collectors steadily raised, to the time when heavy clouds cover sky again (time at 75 min). In real operation of solar system, control unit shuts down circulation pump and thus stops circulation of slowly cooled heat transfer medium. From this reason was electric circulation pump of experimental measuring apparatus stopped. Stopped circulation and low value of solar irradiance caused decrease of thermal power of both solar collectors. A significant difference in the value of thermal power is caused not only by lower temperature of heat transfer medium in ETSC 1-S, but mainly by using a heat exchange chamber made of metal foam in ETSC 2-MF. Heat exchange chamber are able to accumulate heat in metal foam structure and thus keep temperature of heat transfer medium at higher level, e.g. temperature decrease of heat transfer medium in ETSC 2-MF is not as much as it is in ETSC 1-S. After the solar irradiance increased again, electric circulation pump started work immediately and thermal power of both solar collector started to increase. Faster increase of thermal power of ETSC 2-MF can be attributed to inner modification of components configuration of the parallel flow manifold header and therefore to the lower value of liquid volume of manifold header. The smaller liquid volume of manifold header can readily respond to changes of solar irradiance due to the lower value of thermal inertia.

Table 2 depicted summary of presented measurement (TEST 1 to TEST 4). The increase in thermal power of solar collector with proposed manifold header is for all four measurement in the range from 85.2 to  $201.8 \text{ W per } 1 \text{ m}^2$  collector area, respectively the average thermal power increase is  $25.95\% \pm 1.7\%$ .

### 5.1. Performance enhancement factor

Quantification of the actual increase of the solar collector performance was part of comprehensive evaluation of the proposed prototype. Actual increase of the solar collector performance consists not only of increase of heat trans-

**Table 2**

Summary table of representative comparison between ETSC 1-S and ETSC 2-MF.

Mass flow rate ( $\text{kg s}^{-1}$ )	Power per collector area unit ( $\text{W m}^{-2}$ )	Power increase against ETSC 1-S (%)
<i>ETSC 1-S</i>		
0.016	441.2	–
0.033 <sub>clear sky</sub>	611.6	–
0.033 <sub>intermittent cloud covered sky</sub>	95.0	–
0.061	914.3	–
<i>ETSC 2-MF</i>		
0.016	562.7	21.59
0.033 <sub>clear sky</sub>	696.8	12.22
0.033 <sub>intermittent cloud covered sky</sub>	197.3	51.81
0.061	1116.1	18.07

fer performance, but it have to be taking into account also pressure loss of manifold header and thus required power increase of circulation pump resulting from structural modifications and used materials. For this purpose, it can be defined evaluation parameter – performance enhancement factor, which includes both components involved in the overall performance of the device, wherein the heat transfer performance is reduced by the required power increase of circulation pump according to mentioned pressure drop analysis. If we consider fact that standard design of manifold header has in any operating conditions performance enhancement factor 1, value of performance enhancement factor for proposed prototype will be reflected by change of this value. When power of solar collector with proposed manifold header increases, value of performance enhancement factor will be greater than 1, and opposite when power of solar collector decreases, value of performance enhancement factor will be lower than 1. Values of performance enhancement factor during conducted experiments are depicted on Fig. 10.

From Fig. 10 it can be concluded that increase of pressure drop and thus required power increase of circulation pump has only minimal impact on the reduction of overall performance of device. For the mass flow rate of  $0.016 \text{ kg s}^{-1}$  is average performance enhancement factor of proposed solar collector 1.27, for  $0.033 \text{ kg s}^{-1}$  it is 1.14, for  $0.061 \text{ kg s}^{-1}$  it is 1.22 and for experiment with mass flow rate of  $0.033 \text{ kg s}^{-1}$  and intermittent cloud covered sky it is 3.20.

This significant increase of thermal power and performance enhancement factor are caused by several factors, which are results of changes of inner components configuration and used materials of proposed parallel flow manifold header with metal foam structural element. First, the implementation of heat exchange chamber made of metal foam increases interface area between heat pipe condenser and heat transfer medium, e.g. an area involved into heat exchange process. Second, unique pore structure changes flow parameters of heat transfer medium from laminar to turbulent flow, which also increases overall thermal efficiency of heat exchange process. Third, heat accumulation ability of metal foam contributes to increasing heat transfer medium temperature under condition with low solar irradiance. Fourth, the use of blocks made of foam glass, which creates parallel flow channels, decreases inner

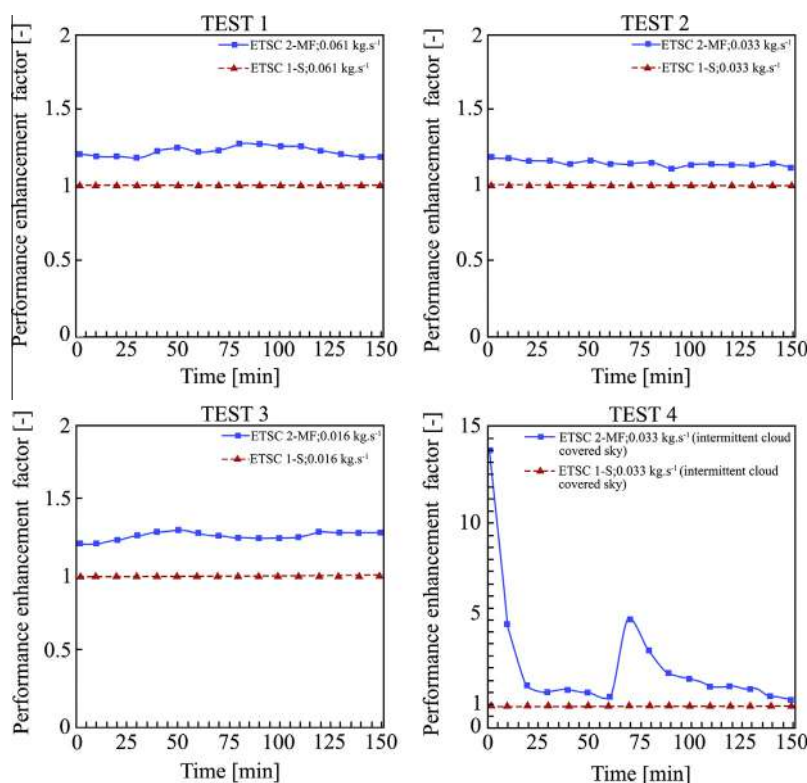


Fig. 10. Summary view of performance enhancement factor for TEST 1 to TEST 4.

liquid volume of manifold header, that positively affect thermal inertia of solar collector. Fifth, parallel flow channel allows to wash each condenser with heat transfer medium at the same temperature, and thus remove same amount of heat and increase heat exchange efficiency. Presented measurement proved the functionality of the new concept, respectively manufactured prototype and in the simple form were able to quantify its contribution to the total heat gain of the solar collectors.

## 6. Conclusions

The presented paper deals with the description of innovation in field of solar collector technology and with method of evaluation of its contribution on overall heat gain. An essential feature of this method is a mutual comparison of thermal power of innovative solar collector and conventional solar collector during simultaneous operation. Measurement of thermal power was performed under quasi dynamic outdoor test conditions on the experimental measuring apparatus designed and manufactured by authors. Appropriateness of the used method of comparison is not only in the low number of necessary measurement instrumentation but especially in low level of measurement error. The final evaluation showed an increase in thermal power of innovated solar collector in the range from 85.2 to 201.8 W on 1 m<sup>2</sup> of collector area and increase of performance enhancement factor in the range from 1.14 to 3.20, that included reduction of heat

transfer performance by the required power increase of circulation pump according to performed pressure drop analysis of proposed prototype of manifold header. Significant increase of thermal power is caused by innovation in form of parallel flow manifold header, which is characterized by use of heat exchange chamber made of metal foam and by changes of inner components configuration of manifold header.

## References

- [1] M. Cehlár, Z. Jurkasová, D. Kudelas, R. Tutko, J. Mendel, Using wood waste in Slovakia and its real energy potential, *Adv. Mater. Res.* 1001 (2014) 131–140, <http://dx.doi.org/10.4028/www.scientific.net/AMR.1001.131>.
- [2] K. Kalaitzakis, E. Koutroulis, V. Vlachos, Development of a data acquisition system for remote monitoring of renewable energy systems, *Measurement* 34 (2003) 75–83, [http://dx.doi.org/10.1016/S0263-2241\(03\)00025-3](http://dx.doi.org/10.1016/S0263-2241(03)00025-3).
- [3] M. Lazzaroni, S. Ferrari, V. Piuri, A. Salman, L. Cristaldi, M. Faifer, Models for solar radiation prediction based on different measurement sites, *Measurement* 63 (2015) 346–363, <http://dx.doi.org/10.1016/j.measurement.2014.11.037>.
- [4] R. Rybár, D. Kudelas, M. Beer, Selected problems of classification of energy sources – what are renewable energy sources?, *Acta Montanistica Slovaca* 20 (2015) 172–180.
- [5] B.B. Ekici, A least squares support vector machine model for prediction of the next day solar insolation for effective use of PV systems, *Measurement* 50 (2014) 255–262, <http://dx.doi.org/10.1016/j.measurement.2014.01.010>.
- [6] P. Tauš, M. Taušová, Economical analysis of PV power plants according installed performance, *Acta Montanistica Slovaca* 14 (2009) 92–97.
- [7] A. Reatti, M.A. Kazimierczuk, M. Catelani, L. Ciani, Monitoring and field data acquisition system for hybrid static concentrator plant,

- Measurement (2015), <http://dx.doi.org/10.1016/j.measurement.2015.06.022> [online 16 September].
- [8] S. Qiu, M. Ruth, S. Ghosh, Evacuated tube collectors: a notable driver behind the solar water heater industry in China, *Renew. Sustain. Energy Rev.* 47 (2015) 580–588, <http://dx.doi.org/10.1016/j.rser.2015.03.067>.
  - [9] M.A. Sabiha, R. Saidur, S. Mekhilef, O. Mahian, Progress and latest developments of evacuated tube solar collectors, *Renew. Sustain. Energy Rev.* 51 (2015) 1038–1054, <http://dx.doi.org/10.1016/j.rser.2015.07.016>.
  - [10] Z.H. Liu, Y.Y. Li, A new frontier of nanofluid research – application of nanofluids in heat pipes, *Int. J. Heat Mass Transfer* 55 (2012) 6786–6797, <http://dx.doi.org/10.1016/j.ijheatmasstransfer.2012.06.086>.
  - [11] H. Peng, J. Li, X. Ling, Study on heat transfer performance of an aluminium flat plate heat pipe with fins in vapour chamber, *Energy Convers. Manage.* 74 (2013) 44–50, <http://dx.doi.org/10.1016/j.enconman.2013.05.004>.
  - [12] K. Chen, S.J. Oh, N.J. Kim, Y.J. Lee, W.G. Chun, Fabrication and testing of a non-glass vacuum-tube collector for solar energy utilization, *Energy* 35 (2010) 2674–2680, <http://dx.doi.org/10.1016/j.energy.2009.05.022>.
  - [13] B. Rassamakin, S. Khairnasov, V. Zaripov, A. Rassamakin, O. Alforova, Aluminium heat pipes applied in solar collectors, *Sol. Energy* 94 (2013) 145–154, <http://dx.doi.org/10.1016/j.solener.2013.04.031>.
  - [14] B.S. Robinson, K.S. Sharp, Heating season performance improvements for a solar heat pipe system, *Sol. Energy* 110 (2014) 39–49, <http://dx.doi.org/10.1016/j.solener.2014.08.042>.
  - [15] M. Moradgholi, S.M. Nowee, I. Abrishamchi, Application of heat pipe in an experimental investigation on a novel photovoltaic/thermal (PV/T) system, *Sol. Energy* 107 (2014) 82–88, <http://dx.doi.org/10.1016/j.solener.2014.05.018>.
  - [16] Y. Deng, Y. Zhao, W. Wang, Z. Quan, L. Wang, D. Yu, Experimental investigation of performance for the novel flat plate solar collector with micro-channel heat pipe array (MHPA-FPC), *Appl. Therm. Eng.* 54 (2013) 440–449, <http://dx.doi.org/10.1016/j.applthermaleng.2013.02.001>.
  - [17] F. Wang, J. Tan, H. Jin, Y. Leng, Thermochemical performance analysis of solar driven CO<sub>2</sub> methane reforming, *Energy* 91 (2015) 645–654, <http://dx.doi.org/10.1016/j.energy.2015.08.080>.
  - [18] F. Wang, J. Tan, Y. Shuai, L. Gong, H. Tan, Numerical analysis of hydrogen production via methane steam reforming in porous media solar thermochemical reactor using concentrated solar irradiation as heat source, *Energy Convers. Manage.* 87 (2014) 956–964, <http://dx.doi.org/10.1016/j.enconman.2014.08.003>.
  - [19] EN 12975-2, Thermal Solar Systems and Components – Solar Collectors – Part 2: Test Methods, European Committee for Standardisation, 2006.
  - [20] ASHRAE 93, ASHRAE Standard 93 Methods of Testing to Determine Thermal Performance of Solar Collectors, American Society of Heating, Refrigerating and Air-Conditioning Engineers, 2003.
  - [21] ISO 9806-1, Test Methods for Solar Collectors. Part 1: Thermal Performance of Glazed Liquid Heating Collectors Including Pressure Drop, International Organization for Standardisation, 1994.
  - [22] GB/T 18708-2002, Test Methods for Thermal Performance of Domestic Solar Water Heating Systems, China Standard Press, 2002.
  - [23] GB/T 19141-2011, Specification of Domestic Solar Water Heating Systems, China Standard Press, 2011.
  - [24] M.A. Sabiha, R. Saidur, S. Hassani, Z. Said, S. Mekhilef, Energy performance of an evacuated tube solar collector using single walled carbon nanotubes nanofluids, *Energy Convers. Manage.* 105 (2015) 1377–1388, <http://dx.doi.org/10.1016/j.enconman.2015.09.009>.
  - [25] M. Hayek, J. Assaf, W. Lteif, Experimental investigation of the performance of evacuated-tube solar collectors under Eastern Mediterranean climatic conditions, *Energy Procedia* 6 (2011) 618–626, <http://dx.doi.org/10.1016/j.egypro.2011.05.071>.
  - [26] G. Colangelo, E. Favale, P. Miglietta, A. de Risi, M. Milanese, D. Laforgia, Experimental test of an innovative high concentration nanofluid solar collector, *Appl. Energy* 154 (2015) 874–881, <http://dx.doi.org/10.1016/j.apenergy.2015.05.031>.
  - [27] R. Liang, J. Zhang, L. Ma, Y. Li, Performance evaluation of new type hybrid photovoltaic/thermal solar collector by experimental study, *Appl. Therm. Eng.* 75 (2015) 487–492, <http://dx.doi.org/10.1016/j.applthermaleng.2014.09.075>.
  - [28] F. Shan, F. Tang, L. Cao, G. Fang, Comparative simulation analyses on dynamic performances of photovoltaic–thermal solar collectors with different configurations, *Energy Convers. Manage.* 87 (2014) 778–786, <http://dx.doi.org/10.1016/j.enconman.2014.07.077>.
  - [29] S.B. Joshi, A.R. Jani, Design, development and testing of a small scale hybrid solar cooker, *Sol. Energy* 122 (2015) 148–155, <http://dx.doi.org/10.1016/j.solener.2015.08.025>.
  - [30] I. Visa, A. Duta, M. Comsit, M. Moldovan, D. Ciobanu, R. Saulescu, B. Burduhos, Design and experimental optimization of a novel flat plate solar thermal collector with trapezoidal shape for facades integration, *Appl. Therm. Eng.* 90 (2015) 432–443, <http://dx.doi.org/10.1016/j.applthermaleng.2015.06.026>.
  - [31] T. Osório, M.J. Carvalho, Testing of solar thermal collectors under transient conditions, *Sol. Energy* 104 (2014) 71–81, <http://dx.doi.org/10.1016/j.egypro.2012.11.148>.
  - [32] B. Du, E. Hu, M. Kolhe, An experimental platform for heat pipe solar collector testing, *Renew. Sustain. Energy Rev.* 17 (2013) 119–125, <http://dx.doi.org/10.1016/j.rser.2012.09.009>.
  - [33] Y. Yang, Y. Wang, W. He, Experimental study of a novel testing platform for the thermal performance of solar domestic water heating systems, *Energy Procedia* 70 (2015) 138–145, <http://dx.doi.org/10.1016/j.egypro.2015.02.109>.
  - [34] E. Mathioulakis, G. Panaras, V. Belessiotis, Uncertainty in estimating the performance of solar thermal systems, *Sol. Energy* 86 (2012) 3450–3459, <http://dx.doi.org/10.1016/j.solener.2012.07.025>.
  - [35] L.M. Ayompe, A. Duffy, Thermal performance analysis of a solar water heating system with heat pipe evacuated tube collector using data from a field trial, *Sol. Energy* 90 (2013) 17–28, <http://dx.doi.org/10.1016/j.solener.2013.01.001>.
  - [36] S. Geddad, G.D. Kumaravel, T. Sivasankar, Determination of thermal performance of a box type solar cooker, *Sol. Energy* 113 (2015) 324–331, <http://dx.doi.org/10.1016/j.solener.2015.01.014>.
  - [37] E. Zambolin, D. Del Col, Experimental analysis of thermal performance of flat plate and evacuated tube solar collectors in stationary standard and daily conditions, *Sol. Energy* 84 (2010) 1382–1396, <http://dx.doi.org/10.1016/j.solener.2010.04.020>.
  - [38] M. Bai, J.N. Chung, Analytical and numerical prediction of heat transfer and pressure drop in open-cell metal foams, *Int. J. Therm. Sci.* 50 (2011) 869–880, <http://dx.doi.org/10.1016/j.ijthermalsci.2011.01.007>.
  - [39] K. Boomsma, D. Poulikakos, F. Zwick, Metal foams as compact high performance heat exchangers, *Mech. Mater.* 35 (2003) 1161–1176, <http://dx.doi.org/10.1016/j.mechmat.2003.02.001>.
  - [40] A. Chumpia, K. Hooman, Performance evaluation of tubular aluminium foam heat exchangers in single row arrays, *Appl. Therm. Eng.* 83 (2015) 121–130, <http://dx.doi.org/10.1016/j.applthermaleng.2015.03.015>.
  - [41] W. Zhou, W. Ling, L. Duan, K.S. Hui, K.N. Hui, Development and tests of loop heat pipe with multi-layer metal foams as wick structure, *Appl. Therm. Eng.* (2015), <http://dx.doi.org/10.1016/j.applthermaleng.2015.10.085> [available online 10 November].
  - [42] R. Dyga, M. Placzek, Heat transfer through metal foam–fluid system, *Exp. Therm. Fluid Sci.* 65 (2015) 1–12, <http://dx.doi.org/10.1016/j.expthermflusci.2015.02.021>.
  - [43] R. Dyga, M. Placzek, Efficiency of heat transfer in heat exchangers with wire mesh packing, *Int. J. Heat Mass Transfer* 53 (2010) 5499–5508, <http://dx.doi.org/10.1016/j.ijheatmasstransfer.2010.07.007>.
  - [44] R. Rybár, D. Kudelas, M. Beer, J. Horodníková, Elimination of thermal bridges in the construction of a flat low-pressure solar collector by means of a vacuum thermal insulation bushing, *J. Solar Energy Eng. Trans. ASME* 137 (2015) 1–4, <http://dx.doi.org/10.1115/1.4030230>.
  - [45] R. Rybár, D. Kudelas, J. Horodníková, M. Beer, Parallel manifold header on foam material basis for vacuum tube solar collectors, *Adv. Sci. Lett.* 19 (2013) 591–594, <http://dx.doi.org/10.1166/asl.2013.4722>.
  - [46] S.J. Kline, F.A. McClintock, Describing uncertainties in single-sample experiments, *Mech. Eng.* (1953) 3–8.